Relation between gas velocity profile and apparent migration velocity in electrostatic precipitators

A. Bäck

GE Power Sweden AB, P.O. Box 1233, SE-351 12, Växjö, Sweden
Corresponding author: *andreas.back@ge.com*

Abstract The impact of the gas velocity profile on the collection efficiency for electrostatic precipitators is considered from a theoretical point of view. If non-ideal effects such as rapping, re-entrainment and gas sneakage are neglected, the maximum collection efficiency is obtained with a perfectly uniform velocity profile throughout the precipitator. Employing a linearization of the exponential function in the equation for collection efficiency, a closed form analytical expression for the impact of non-uniform gas flow is derived. In the expression, the square of the coefficient of variation of the gas flow profile enters as a correction factor to the migration velocity. The analytical expression corresponds rather well to exact calculations on actual gas velocity distributions, up to coefficient of variations around 30%. Moreover, it is demonstrated that the same type of approach can be used to derive similar correction factors also when other variables deviate from uniformity.

Keywords: Electrostatic Precipitator, ESP, Gas Distribution, Coefficient of Variation, Migration Velocity

1. Introduction

The gas flow distribution is one of the parameters that affect the efficiency of an electrostatic precipitator (ESP). In fact, the global flow pattern and velocity distribution of the gas inside the ESP casing is one of the factors that must be considered from the design phase all the way through commissioning, tuning and performance testing, as well as in various upgrade scenarios [1-11]. In addition to the global flow pattern, there is also the corona-generated electro hydrodynamic flow (EHD flow) in the inter-electrode region, which may affect for example the selection of electrode geometry [12-15].

This article will focus on the global flow profile in the ESP and its direct impact on the dust collection efficiency. With "direct impact" on performance we here mean the impact when neglecting all non-ideal effects in the ESP that may be affected by the gas velocity. This includes for example gas sneakage, dust re-entrainment, rapping losses, gravimetric settling, and corona suppression. A more stringent way of saying that no non-ideal effect will be considered is to state that only the Deutsch equation will be used in the analysis. In this way the gas velocity only enters as the inverse of the treatment time of the flue gas in the electric field, and no non-ideal effects are added as extra terms or correction factors. Of course, the details of the EHD flow in the inter-electrode gaps are not considered by the Deutsch equation, except that the turbulence is implicitly assumed to accomplish ideal mixing of the dust along the width of each gas passage in the ESP.

In the analysis below, a non-uniform gas velocity distribution will be assumed throughout the entire length of the ESP, and the effect on outlet emission is compared to the case with a completely even flow profile. As remarked above, this will be conducted in a completely idealized "Deutschian" analysis, although the somewhat more general Matts-Öhnfeldt equation (modified Deutsch equation) will be used. This adds little to the complexity and includes the ordinary Deutsch equation as a special case.

2. Analysis of non-uniform gas velocity profile

Although it is established that the velocity profile inside an ESP must be tuned in order to reach the highest possible performance, there is no consensus on the exact shape of flow profile that minimizes the emission. For example, significant efforts have been made to investigate so-called skewed gas flow, which is a deliberate skew of the gas velocity profile in order to optimize the ESP performance [16-19]. Even if application of various types of non-uniform and skewed flow profiles has a potential for emission reduction in many cases, the exact details of the optimum flow may vary depending on process conditions and type of dust. Nevertheless, it is generally accepted that gas sneakage below and above the fields must be avoided in any scenario, and that local high velocities inside the ESP fields may reduce the overall performance substantially. Also, it is clear that from theoretical point of view and under ideal conditions the best overall dust collection efficiency is achieved with a completely uniform gas distribution. Any deviation from the perfect uniform velocity profile will then lead to a reduced efficiency and a corresponding increase in outlet dust concentration.

Even if model testing or CFD has been performed in the planning and design phase, it is common to measure and adjust the gas velocity inside the ESP during commissioning. Typically, the gas velocity is measured with an anemometer at several elevations (e.g. one point per meter) in each gas passage of the ESP (or every second gas passage), such that the entire cross section is mapped. This can, if needed, be done in several planes along the length of the ESP, but

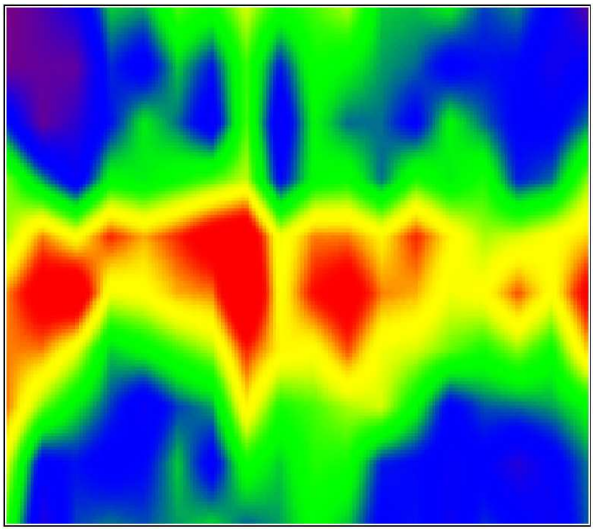

Figure 1. Measured velocity profile after the first field in an ESP at a pelletizing plant. Red color corresponds to the highest velocity, followed by yellow, green, blue and purple

for practical reasons a gas distribution measurement is often limited to only one plane. The result of a gas velocity distribution measurement after the first field in an ESP may look as in Fig. 1.

A suitable and frequently used measure of the uniformity of the cross sectional gas flow profile in an ESP is the Coefficient of Variation (CV) [2-7,10]. The CV is defined as the ratio of the standard deviation to the mean, i.e.

$$\mathrm{CV}=\frac{\sigma}{\bar{v}}=\frac{1}{\bar{v}}\sqrt{\frac{\sum_{n=1}^{N}(v_n-\bar{v})^2}{N}}\,, \qquad (1)$$

with $\bar{v}$ being the average gas velocity in the ESP:

$$\bar{v}=\frac{\sum_{n=1}^{N} v_n}{N}\,. \qquad (2)$$

The set of measured gas velocities in all points of the cross-section v_1, v_2, … v_n,… v_N can of course be analysed in several ways to obtain a criteria for the quality of the gas flow profile. For example, the publication EP-7 by ICAC (Institute of Clean Air Companies) specifies that 85% of the measured velocities in a cross-section shall be less than 1.15 times the average velocity and 99% below 1.40 [20]. The ICAC criterion is, however, often interpreted as a limitation of the maximum allowed CV-value to 15% (which results if a Gaussian distribution of velocities around the mean is assumed).

Now the impact of a non-uniform gas flow profile on the dust emission from an ESP will be evaluated. The most straightforward approach is of course to calculate the emission from each sub-area of the cross-section with its measured velocity and to sum up all contributions. This is easily accomplished numerically, but an approximate closed form expression would anyhow be desirable for increased understanding and convenience. As stated above, the analysis will be based on the Matts-Öhnfeldt equation, which is a generalized form of the ordinary Deutsch equation [21]. The relation between inlet and outlet dust concentration is obtained via the migration velocity, w_k, the ESP collecting area, A, and the flue gas flow rate, Q:

$$C_{out}=C_{in}\exp[-(w_kA/Q)^k]\,. \qquad (3)$$

The parameter k allows an ad hoc adjustment of the equation, mainly to compensate for different particle size distributions of the incoming dust. Often the rather broad fly ash size distribution from e.g. coal-fired boilers corresponds to k-values around 0.5, while $k=1$ corresponds to a uniform particle size and is identical to the original Deutsch equation. Alternatively, Eq. (3) can be expressed in terms of gas velocity, v, rather than the gas flow rate, Q, viz.,

$$C_{out}=C_{in}\exp\left[-\left(w_k\frac{L}{rv}\right)^k\right], \qquad (4)$$

where L is the length of the ESP and r is the distance between discharge electrode and collecting plate for the case of a duct-type precipitator. In the normal case, the gas velocity v would simply be the average gas velocity, $\bar{v}$. In the analysis of the influence of an uneven velocity profile in the ESP, it is practical to work with the mass flow of dust rather than the dust concentration. Thus we multiply both sides of Eq. (4) with the gas flow Q. Noting that $Q = Bv$, where B is the cross section area of the ESP, we get:

$$\dot{m}_{out}=QC_{out}=BvC_{out}=BvC_{in}\exp\left[-\left(w_k\frac{L}{rv}\right)^k\right]. \qquad (5)$$

We now divide the cross section of the ESP into several smaller areas, B_n, each with its own gas velocity, v_n, and sum over all paths to obtain the total mass flow for a non-uniform flow profile:

$$\dot{m}_{out}=\sum_{n=1}^{N}\dot{m}_{out,n}=\sum_{n=1}^{N}B_nv_nC_{in}\exp\left[-\left(w_k\frac{L}{rv_n}\right)^k\right]. \qquad (6)$$

It is important to understand that the lower overall ESP collection efficiency at a non-uniform gas flow depends on two independent factors: The non-linear character of the exponential function and the weighted averaging procedure. For relatively small velocity variations and if the collection efficiency is not extremely high, the later factor dominates, such that a reasonable approximation may be obtained via a linearization of the exponential. Therefore, the next step is to make a first order Taylor expansion of the exponential around the average velocity:

$$\exp\left[-\left(\frac{w_kL}{rv_n}\right)^k\right]\approx\exp\left[-\left(\frac{w_kL}{r\bar{v}}\right)^k\right]\left(1+k\left(\frac{w_kL}{r\bar{v}}\right)^k\frac{(v_n-\bar{v})}{\bar{v}}\right). \qquad (7)$$

Combining Eq. (7) with Eq. (6), and assuming that all sub-areas, B_n, are equal ($B_n = B/N$) we obtain:

$$\dot{m}_{out} \approx C_{in}\frac{B}{N}\sum_{n=1}^{N} v_n\left(1+k\left(\frac{w_k L}{r\bar{v}}\right)^k\frac{(v_n-\bar{v})}{\bar{v}}\right)\exp\left[-\left(w_k\frac{L}{r\bar{v}}\right)^k\right]. \quad (8)$$

Lifting the constant exponential factor outside the summation and splitting the sum into two parts yields:

$$\begin{aligned}&\dot{m}_{out} \approx\\ &C_{in}\frac{B}{N}\exp\left[-\left(w_k\frac{L}{r\bar{v}}\right)^k\right]\sum_{n=1}^{N} v_n +\\ &C_{in}\frac{B}{N}\exp\left[-\left(w_k\frac{L}{r\bar{v}}\right)^k\right]\sum_{n=1}^{N} k\left(\frac{w_k L}{r\bar{v}}\right)^k\frac{(v_n-\bar{v})}{\bar{v}}v_n\,. \end{aligned} \quad (9)$$

The first term on the right side of Eq. (9) represents the total outlet mass flow of dust at uniform face velocity, $\bar{v}$, i.e. what we may call our "base case emission" $\bar{\dot{m}} = QC_{out} = B\bar{v}C_{in}\exp[-(w_k L/r\bar{v})]$. The second term on the right side of Eq. (9) is then the extra emission of dust due to having a non-uniform velocity profile. Using the substitution $v_n = (v_n - \bar{v}) + \bar{v}$, we can convert the second term into a quadratic term plus an extra term that becomes zero, viz.,

$$\begin{aligned}&C_{in}\frac{B}{N}\exp\left[-\left(w_k\frac{L}{r\bar{v}}\right)^k\right]\sum_{n=1}^{N} k\left(\frac{w_k L}{r\bar{v}}\right)^k\frac{(v_n-\bar{v})}{\bar{v}}v_n =\\ &C_{in}\frac{B}{N}\exp\left[-\left(w_k\frac{L}{r\bar{v}}\right)^k\right]\sum_{n=1}^{N} k\left(\frac{w_k L}{r\bar{v}}\right)^k\frac{(v_n-\bar{v})^2}{\bar{v}} +\\ &C_{in}\frac{B}{N}\exp\left[-\left(w_k\frac{L}{r\bar{v}}\right)^k\right]\sum_{n=1}^{N} k\left(\frac{w_k L}{r\bar{v}}\right)^k\frac{(v_n-\bar{v})\bar{v}}{\bar{v}}. \end{aligned} \quad (10)$$

With the last sum being identical to zero on account of being "the average deviation from the average", we insert Eq. (10) into Eq. (9) and arrive at the final expression after some reshuffling:

$$\begin{aligned}&\dot{m}_{out} \approx\\ &C_{in}B\bar{v}\exp\left[-\left(w_k\frac{L}{r\bar{v}}\right)^k\right] +\\ &C_{in}B\bar{v}\exp\left[-\left(w_k\frac{L}{r\bar{v}}\right)^k\right]k\left(\frac{w_k L}{r\bar{v}}\right)^k\frac{1}{N}\sum_{n=1}^{N}\frac{(v_n-\bar{v})^2}{\bar{v}^2}. \end{aligned} \quad (11)$$

Denoting again the base emission at uniform gas velocity, $\bar{v}$, as $\bar{\dot{m}}$ (equal to $B\bar{v}C_{in}\exp[-(w_k L/r\bar{v})]$) and with the definition of CV from Eq. (1), we may write:

$$\dot{m}_{out} \approx \bar{\dot{m}}\left(1+k\left(\frac{w_k L}{r\bar{v}}\right)^k(\mathrm{CV})^2\right). \quad (12)$$

In other words, Eq. (12) says that the emission with a non-uniform gas flow is (approximately) equal to the base emission at uniform velocity, plus a term that is proportional to the square of the variation coefficient of the flow profile.

While the expression for the increase in emission according to Eq. (12) is basically the relation sought at the outset of the analysis, it may be of more value to obtain a direct correlation between CV and w_k. This is possible via the approximation of interpreting the parenthesis in Eq. (12) as a Maclaurin expansion of an exponential function, i.e.

$$\left(1+k\left(\frac{w_k L}{r\bar{v}}\right)^k(\mathrm{CV})^2\right) \approx \exp\left[k\left(\frac{w_k L}{r\bar{v}}\right)^k(\mathrm{CV})^2\right]. \quad (13)$$

Combining Eq. (13) with Eq. (12), and introducing the explicit expression for $\bar{\dot{m}}$, yields:

$$\begin{aligned}&\dot{m}_{out} \approx \bar{\dot{m}}\exp\left[k\left(\frac{w_k L}{r\bar{v}}\right)^k(\mathrm{CV})^2\right] =\\ &C_{in}B\bar{v}\exp\left[-\left(\frac{w_k L}{r\bar{v}}\right)^k\right]\exp\left[k\left(\frac{w_k L}{r\bar{v}}\right)^k(\mathrm{CV})^2\right] =\\ &C_{in}B\bar{v}\exp\left[-\left(\frac{w_k L}{r\bar{v}}\right)^k\left(1\text{-}k(\mathrm{CV})^2\right)\right] =\\ &C_{in}B\bar{v}\exp\left[-\left(\left(w_k\left(1\text{-}k(\mathrm{CV})^2\right)^{1/k}\right)\frac{L}{r\bar{v}}\right)^k\right], \end{aligned} \quad (14)$$

so that the change in emission is expressed via a correction factor multiplying w_k. As an alternative, it is of course also possible to convert the final form of Eq. (14) back to the more usual type based on dust concentrations and specific collecting area, viz.,

$$C_{out} \approx C_{in}\exp\left[-\left(\left[w_k(1-k(\mathrm{CV})^2)^{1/k}\right]A/Q\right)^k\right]. \quad (15)$$

The correction factor for non-uniform gas flow in the ESP, $(1\text{-}k(\mathrm{CV})^2)^{1/k}$, which reduces the apparent migration velocity, can be simplified one step further via the approximation $(1\text{-}a\varepsilon)^{1/a} \approx (1\text{-}\varepsilon)$. This relation is valid for any value of the parameter a, if ε is small enough, which is basically always the case for our application where $(\mathrm{CV})^2$ would rarely be higher than 0.1 or thereabout. The final expression is then:

$$C_{out} \approx C_{in}\exp[-([w_k(1-(\mathrm{CV})^2)]A/Q)^k]. \quad (16)$$

Using Eq. (16), the effect of non-uniform gas velocity in an ESP can now be evaluated for various cases. For example, the ICAC criteria from Ref. [20] that limits the velocity CV to max 15%, gives at most a correction factor of 0.9775 (i.e. $1-0.15^2$). Another example is the optimum velocity profile specified for ESPs supplied by GE, where the test points in top and bottom of the precipitator should ideally have 85% of the average velocity, while all other points "in the middle" should have a uniform distribution. With a 15m tall ESP we may then have one point in the top and one point in the bottom of each gas duct with velocity 0.85 m/s, and 13 points in the middle with 1.023 m/s. This corresponds to a CV of 5.9%, giving an almost negligible correction factor of 0.9965 for w_k. Such an offset is certainly very small compared to the possible gain by reduced gas sneakage above and below the ESP fields. As a final example we may take two parallel ESP casings after a boiler, each with perfectly uniform gas velocity profile, but where one casing handles 55% of the total gas flow and the other casing 45%. This gives an overall CV of 10%, and consequently a correction factor of 0.99 for the apparent migration velocity.

The examples above are rather illustrative and provide an intuitive feeling of the approximate relative impact of a non-ideal velocity profile. However, it must still be remembered that the analysis rests on some significant simplifications. In addition to the ideal treatment, one major simplification is the assumption that the gas flow profile does not change along the length of the ESP, which is not true in reality. Then there is also the question about the size of the error

committed in the derivation of the correction factor in Eq. (16) due to the linearization employed. This issue will be investigated below, by comparing the approximate correction factor with its numerically calculated counterpart for some actual cases.

To investigate the accuracy of the approximate correction factor $(1-(CV)^2)$ from Eq. (16), we shall use some actual measured gas velocity profiles in a number of ESPs for various processes, operating at different collection efficiencies. For the analysis we will utilize measured velocity profiles in six different ESPs, before- and after adjustment/optimization of the flow. For each ESP the value of CV is calculated from the set of measured velocities in the cross-section after the first field. The same set of velocities is also used to numerically calculate the emission for each sub-area with its own velocity, using the Matts-Öhnfeldt equation, according to Eq. (6). The so obtained emission is converted to a corresponding overall migration velocity, w_k, for the entire ESP. This "global" apparent migration velocity is then compared with the original migration velocity, which was used for all sub-areas, to obtain the correction factor. In the calculations the actual parameters of each ESP has been used, including the assumed base migration velocities that result in emissions and collection efficiencies agreeing well with reality.

The six precipitators are: ESP for sinter band fat gases with collection efficiency (η) of 96.9%; ESP at a pelletizing plant with $\eta = 99.86\%$; ESP after oil shale fired CFB boiler with $\eta = 99.94\%$; ESP after boiler firing lignite with $\eta = 99.87\%$; ESP after boiler firing hard coal with $\eta = 99.56\%$; ESP downstream a soda recovery boiler with $\eta = 99.82\%$. The calculations for the five first ESPs were made with a value of the *k*-parameter in the Matts-Öhnfeldt equation equal to the classical value of 0.5, while the soda recovery boiler application used the value of 1. Taking a *k*-value close to unity is representative for a uniform or very narrow size distribution, which may here be taken as a reasonable approximation for the dust from a soda recovery boiler. In Fig. 2 the numerical results for each of the six ESPs are shown – obtained by using the Matts-Öhnfeldt formula for each sub-area of the ESP cross-section with its own velocity.

Each ESP is represented by two identical symbols in Fig. 2, where the one with higher value of CV corresponds to the original velocity profile, before any adjustment of the gas distribution. Then the symbol with lower CV is the calculation using the improved velocity profile after modifications to the ESP screens and/or inlet duct. The approximate correction factor, $(1-(CV)^2)$, from the analytical derivation, is plotted as a solid black line in the figure. It is readily seen that the agreement between an exact numerical treatment and the approximate analytical correction factor is excellent for the case of the sinter band ESP, which works at the lowest collection efficiency (96.9%). For the other cases, the agreement declines with increasing CV, especially for the precipitators having the highest

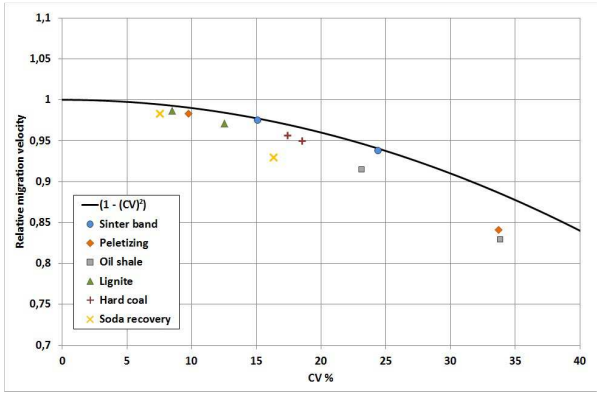

Figure 2. Approximate correction factor for non-uniform gas flow versus numerical calculations for several actual examples of ESP gas velocity distributions

collection efficiencies. The case of the soda recovery boiler shows a particularly poor agreement, demonstrating that a high *k*-value leads to an increasing error in the linearization of the exponential function, which is the basis of the derivation of the analytical correction factor. Nevertheless, the general behavior of the exact calculations corresponds rather well with the curve from the analytical treatment, and in reality the fact that the gas distribution typically gets progressively better along the length of the ESP will likely cover part of the deviation, if the exact results fall below the line. Furthermore, it is not inconceivable that retaining the general parabolic curve shape while introducing an empirical fitting parameter (that depends on η, *k*, and possibly on CV) may lead to a more accurate expression, which still has a relatively simple form.

3. Application to electrode misalignment

It is worthwhile to investigate whether the analysis developed in the previous section can be used for other imperfections of an ESP than the non-uniformity of the gas velocity profile. The approach to arrive at the correction factor for w_k in Eq. (16) was rather general, and based on the principle that in the averaging procedure the paths in the ESP having lower efficiency also carry a higher weight (i.e. amount of dust). We shall try to generalize the approach as much as possible in the next section, but in this section we will begin with a virtually identical analysis as for the non-uniform gas flow, for the case of misalignment of the ESP electrodes.

The start of our analysis will be Eq. (6), which carries over completely unchanged from the derivation concerning non-uniform gas velocity. For Eq. (6) we now apply an opposite approach, namely that it is the sub-areas, B_n, that are all different, while all velocities, v_n, are identical ($v_1 = v_2 = \ldots = v_n = \ldots = \bar{v}$). The definition of the sub-areas in the ESP cross-section is explained by Fig. 3. Due to displacement and misalignment of various discharge- and collecting electrodes (exaggerated in the figure for clarity), not all sub-areas are equal. Ideally, in a perfectly built ESP, all subsections would have an area equal to half the spacing multi-

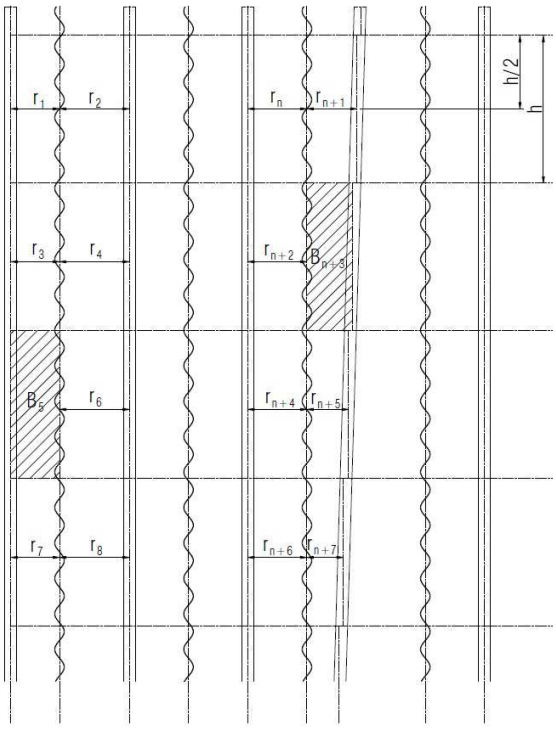

Figure 3. Definition of distances and areas in an ESP field with misalignment in the electrode system

plied by the height of the measurement grid, i.e. $B_1 = B_2 = \ldots = B_n = \ldots = B_N = rh$. Now instead, due to the varying distances between discharge and collecting electrodes, we have $B_1 = r_1 h$, $B_2 = r_2 h$, … , $B_n = r_n h$, $B_{n+1} = r_{n+1} h$, …, which means that larger amount of gas passes in the sub-areas where the distance between the electrodes is largest. The portions with large electrode distance are also where the gas cleaning is least efficient, due to lower electric field and current (and longer average distance for the particles to travel). Using the principles outlined above, we now re-state Eq. (6), but with varying areas and constant gas velocity:

$$\dot{m}_{out} = \sum_{n=1}^{N} \dot{m}_{out,n} = \sum_{n=1}^{N} r_n h v C_{in} \exp\left[-\left(w_k \frac{L}{r_n v}\right)^k\right], \quad (17)$$

where we have used the notation v rather than $\bar{v}$ for the constant gas velocity. It is clear that Eq. (17) is completely analogue to Eq. (6), so that the derivation will proceed in exactly the same way as in Sec. 2. Thus, we arrive to the following expression, which is the analogue of Eq. (11):

$$\dot{m}_{out} \approx C_{in} B v \exp\left[-\left(w_k \frac{L}{\bar{r} v}\right)^k\right] + C_{in} B v \exp\left[-\left(w_k \frac{L}{\bar{r} v}\right)^k\right] k \left(\frac{w_k L}{\bar{r} v}\right)^k \frac{1}{N} \sum_{n=1}^{N} \frac{(r_n - \bar{r})^2}{\bar{r}^2}. \quad (18)$$

Here the value $\bar{r}$, around which we have performed the Taylor expansion, is the average distance between discharge electrodes and collecting plates (which of course is half the nominal plate-to-plate spacing). To continue the analysis we define the coefficient of variation for the electrode alignment in exactly the same fashion as for velocity profile, i.e.

$$\mathrm{CV_a} = \frac{\sigma}{\bar{r}} = \frac{1}{\bar{r}} \sqrt{\frac{\sum_{n=1}^{N} (r_n - \bar{r})^2}{N}}, \quad (19)$$

where we have added the subscript "a" to separate the alignment-CV from the velocity-CV. We immediately recognize that the last factor in the second term of Eq. (18) is equal to $(\mathrm{CV_a})^2$, and continue the derivation. Just as in Sec. 2, we reach expressions for the increased emission and decreased migration velocity as

$$\dot{m}_{out} \approx \bar{\dot{m}} \left(1 + k \left(\frac{w_k L}{\bar{r} v}\right)^k (\mathrm{CV_a})^2\right) \quad (20)$$

and

$$C_{out} \approx C_{in} \exp[-([w_k (1 - (\mathrm{CV_a})^2)] A/Q)^k]. \quad (21)$$

Focusing on the correction factor for the migration velocity, $(1\text{-}(\mathrm{CV_a})^2)$, which may be considered as the main result, an actual example may be useful. Suppose that the tolerances for electrode alignment have been measured in each gas passage at several elevations. The outcome may be a protocol that could look something like Fig. 3, but larger and with actual numbers filled in. In an ESP with 400 mm spacing the value of r_1, r_3, r_5, r_7, etc. could be, for example, 180 mm. On the other half of the same duct the distances are then correspondingly longer at 220 mm. In another location one of the collecting plates may not be perfectly vertical (as the fourth plate from left in Fig. 3), giving a new set of measured distances. Many other electrode rows may be found to be nearly perfect, giving many distances of 200 mm. By way of example, say that 50% of the distances were found to be the nominal 200 mm, while 15% + 15% were 210 mm and 190 mm, respectively, and finally 6% + 6% at 220 mm / 180 mm and 4% + 4% at 230 mm / 170 mm. Such a result corresponds to a $\mathrm{CV_a}$ of 6.1%, according to Eq. (19). The corresponding correction factor for the migration velocity, $(1\text{-}(\mathrm{CV_a})^2)$, becomes 0.9963. This result would indicate that an electrode misalignment of up to ±30 mm in some gas passages of a 400 mm spacing ESP would have almost negligible impact on its performance. Even more so since the same misalignment would not extend all the way through the precipitator casing in a multi-field ESP. However, the analysis in this section has only considered the ordinary $1/r$ dependence of the exponential in the Matts-Öhnfeldt modified Deutsch equation. This is certainly an underestimation, as will be discussed in the next section, where a more realistic approach is implemented.

4. Generalization of the linearized non-uniformity correction

The goal of this section is to make a generalization of the analysis in the previous two sections, and to apply the result on a more realistic model for the effect of electrode misalignment. Still, the approach is only of approximate nature, but will be more qualitatively correct and may help with increased understanding and simple order of magnitude estimates.

Considering the analysis in Sec. 2 and Sec. 3, where the dependence of the non-uniform variable inside the exponential was in both cases of the form $1/x$, it seems plausible to investigate if the form $1/x^q$ leads to similar results. Our starting point will therefore be a relation of the type:

$$\dot{m}_{out} = \sum_{n=1}^{N} \dot{m}_{out,n} = \sum_{n=1}^{N} p x_n \exp\left[-\left(\frac{g}{x_n^q}\right)^k\right], \quad (22)$$

where p, g and q are constants. For example in Sec. 2, where "x" was the velocity v, we had the constant p equal to $C_{in}B/N$ and g was w_kL/r, while q was of course equal to unity. The Taylor expansion to first order of the exponential in Eq. (22) results in an expression very similar to Eq. (7) above:

$$\exp\left[-\left(\frac{g}{(x_n)^q}\right)^k\right] \approx \exp\left[-\left(\frac{g}{(\bar{x})^q}\right)^k\right]\left(1 + kq\left(\frac{g}{(\bar{x})^q}\right)^k \frac{(x_n-\bar{x})}{(\bar{x})}\right), \quad (23)$$

where the expansion is again made around the average value of the parameter (i.e. $\bar{x} = \sum_{n=1}^{N} x_n/N$). Using Eq. (23) in Eq. (22), and continuing as in Sec. 2 and Sec. 3, it is easy to see that the same type of expressions will be obtained in every step. This since the only difference between Eq. (23) and Eq. (7) is the constant factors. Thus we obtain the equivalent of Eq. (11) as

$$\dot{m}_{out} \approx pN\bar{x}\exp\left[-\left(\frac{g}{(\bar{x})^q}\right)^k\right] + pN\bar{x}\exp\left[-\left(\frac{g}{(\bar{x})^q}\right)^k\right] kq\left(\frac{g}{(\bar{x})^q}\right)^k \frac{1}{N}\sum_{n=1}^{N}\frac{(x_n-\bar{x})^2}{(\bar{x})^2}. \quad (24)$$

With notations as before, and recognizing the squared coefficient of variation for the parameter x in the last term, formulas for the emission are obtained as

$$\dot{m}_{out} \approx \bar{\dot{m}}\left(1 + kq\left(\frac{g}{(\bar{x})^q}\right)^k (\mathrm{CV})^2\right) \quad (25)$$

and

$$C_{out} \approx C_{in}\exp\left[-\left(\left[g\left(1\text{-}q(\mathrm{CV})^2\right)\right]/(\bar{x})^q\right)^k\right]. \quad (26)$$

These final expressions show that the generalization of the analysis in Sec. 2 and Sec. 3 to a dependence where the non-uniform parameter in the denominator is raised to an arbitrary power, results in the same type of correction factors. The only difference is the multiplication of the squared CV-value by the exponent q, giving a more significant correction for large values of q, and vice versa.

We will now utilize this new result to develop the analysis in Sec. 3 to obtain a somewhat more realistic approach for the effect of non-perfect electrode alignment. Again we divide the precipitator cross-section in many sub-areas, as per Fig. 3. Due to misalignment of the electrodes the areas are different, and have different distance between discharge electrode and collecting plate. This also means that the electric field strength will be different in each sub-area. If the precipitator operating voltage is U, then the average electric field in a given half-duct subsection with distance r between discharge- and collecting electrode may be defined as U/r. We now draw our attention to the classical theoretical formula for the Deutsch migration velocity [1-3]:

$$w = w_k\{k=1\} = \frac{2\varepsilon_r}{\varepsilon_r+2}\frac{\varepsilon_0 E_0 E_p a}{\mu}, \quad (27)$$

where E_0 is the charging electrical field and E_p is the precipitation field strength. We define a new constant, γ, containing the particle radius a and the dynamic viscosity μ, as well as the vacuum permittivity and dielectric constant of the particles:

$$w = \gamma E_0 E_p. \quad (28)$$

Then we assume that both the charging- and precipitating electrical field strengths are proportional to the average field strength $\bar{E} = U/r$, such that

$$w = \gamma E_0 E_p \approx \xi \bar{E}\bar{E} = \xi\frac{U^2}{r^2}. \quad (29)$$

We next assume that the same type of approximate expression is valid also for the modified migration velocity, w_k, i.e.

$$w_k \approx \xi_k \frac{U^2}{r^2}, \quad (30)$$

where the constant ξ_k may depend on the value of the k-parameter in the Matts-Öhnfeldt equation.

Before combining the results from this section with Eq. (17) from Sec. 3, we must first make clear that the misalignment of the electrodes in an ESP affects the performance via two mechanisms. The first is the one that was in principle covered in Sec. 3 (and that will be refined in this section), namely that the largest sub-areas has the longest distance between the electrodes, and therefore lower collection efficiency. The second factor is that the maximum voltage which can be reached in an ESP section (before sparking) is depending on the minimum distance between discharge electrode and collecting plate at any location in that section. These two effects may be taken care of independently in the analysis. To cover for the effect of premature sparking due to some minimum electrode

distance, we assume that the maximum voltage, U, that can be achieved in the section is

$$U = \frac{r_{min}}{\bar{r}} U_{nom} \,, \qquad (31)$$

where r_{min} is the minimum electrode distance at any location in the section. The ideal maximum voltage, U_{nom}, is the voltage at sparking if the entire system was perfectly aligned with the electrode distance equal to $\bar{r}$ (half nominal plate spacing) at all locations.

Now we insert the expression for the migration velocity obtained in Eq. (30) into Eq. (17) to get:

$$\dot{m}_{out} = \sum_{n=1}^{N} r_n h v C_{in} \exp\left[-\left(\xi_k \frac{U^2}{r_n^2} \frac{L}{r_n v}\right)^k\right]. \qquad (32)$$

The form of Eq. (32) is that of Eq. (22) with $q = 3$, so that we will be able to use the results derived in the beginning of this section. Identifying coefficients we get $p = hvC_{in}$, $g = \xi_k U^2 L/v$ and $q = 3$. Following the analysis above (i.e. from Eq. (22) to Eq. (26)), we obtain:

$$C_{out} \approx C_{in} \exp\left[-\left(\left[\frac{\xi_k U^2 L}{v}\left(1\text{-}3(\mathrm{CV_a})^2\right)\right]/(\bar{r})^3\right)^k\right]. \qquad (33)$$

Recalling Eq. (31), compensating for lower achievable voltage due to some minimum distance between discharge electrode and collecting plate, we have the final result:

$$C_{out} \approx C_{in} \exp\left[-\left(\left[\frac{\xi_k U_{nom}^2 r_{min}^2 L}{v(\bar{r})^2}\left(1\text{-}3(\mathrm{CV_a})^2\right)\right]/(\bar{r})^3\right)^k\right]. \qquad (34)$$

We may alternatively hide the details by using the relation for w_k in Eq. (30) at an ideal geometry, i.e. $w_k = \xi_k U_{nom}^2/(\bar{r})^2$, and express in terms of A/Q rather than L/rv:

$$C_{out} \approx C_{in} \exp\left[-\left(\left[w_k \frac{r_{min}^2}{(\bar{r})^2}\left(1\text{-}3(\mathrm{CV_a})^2\right)\right] A/Q\right)^k\right]. \qquad (35)$$

This is the approximate equation for the impact of misaligned electrodes. The two correction factors for w_k are clearly separated – One for premature sparking and the other for the coefficient of variation for the mialignment (due to larger gas flow passing in regions with the weakest electric field).

Taking the same example as in Sec. 3 of a somewhat misaligned electrode system, we can compare the outcome of Eq. (35) with the simpler treatment leading up to Eq. (21). The situation was an electrode system with nominal 400 mm plate-to-plate distance, where 50% of the electrode distances were perfectly aligned, while 30% deviated ±10 mm, 12% deviated ±20 mm and 8% deviated ±30 mm. This gave a coefficient of variation for electrode alignment, $\mathrm{CV_a}$ = 6.12%, and correspondingly a value for $(\mathrm{CV_a})^2$ of 0.00375. In Eq. (35) this leads to a correction factor of $(1\text{-}3(\mathrm{CV_a})^2) = 0.98875$, which is still a rather moderate reduction of performance. On the other hand, the correction for reduced maximum voltage due to sparking at the shortest electrode distance becomes $r_{min}^2/\bar{r}^2 = 170^2/200^2 = 0.7225$, which is a much stronger offset indeed. Thus, it is demonstrated that the main problem of electrode misalignment is related to the premature sparking due to the minimum electrode clearance of the field. As a consequence, it is also clear that the performance impact of misalignment is significantly less for an ESP operating below the sparking limit (e.g. to manage a power consumption guarantee). However, even if the CV-based correction factor is rather limited in the example provided, it may in reality be larger than indicated by the simplified analytic expression. Partly this is because the linearization underestimates the true impact rather significantly for high values of q and at high collection efficiencies. It is also due to the displacement of current density that follows from the misalignment, which has not been considered in our analysis. But even if these factors are considered, the effect of sparking at lower voltage will dominate in most cases. This is especially true for multi-field ESPs, where the same misalignment pattern is very unlikely to extend through the entire length of the ESP.

5. Conclusions

It has been shown that a non-uniform gas velocity profile in the cross-section of an ESP results in a decrease of the apparent migration velocity, with correspondingly higher emission of dust. More precisely, a first order Taylor expansion of the exponential in the Matts-Öhnfeldt equation is utilized to obtain an approximate analytical expression for the reduction of the migration velocity, w_k. The correction factor multiplying w_k is of the form $(1\text{-}(\mathrm{CV})^2)$, where CV is the coefficient of variation for the velocity profile in the ESP cross-section. Comparison with an exact summation of all individual emissions for the paths of different velocities, shows that the agreement is very good for moderate collection efficiencies and at least semi-quantitative for high efficiencies. The appearance of the CV-value in a simple and relatively accurate correction factor is an incentive for its use as a suitable measure for gas flow quality. Furthermore, since the correction factor is always less than unity, it proves that a completely uniform gas flow gives the highest performance in an ESP under ideal conditions. This proof is mathematically strict, since the linearizations in the derivation become exact as CV tends towards zero.

It was also demonstrated that the method used for analysis of non-uniform gas flow may be generalized and applied to e.g. the case of misaligned electrode geometry in an ESP. For the misalignment, a similar type of CV-based correction factor results, and in addition a much stronger correction factor for the reduced maximum voltage enters the expression. From this it can be concluded that the tolerances for electrode alignment are much more critical for an ESP operating under spark-limited conditions, where some

minimum electrode distance can reduce the operating voltage of the whole field.

As a final comment, it should again be stressed that the results in this paper are derived under the assumption of ideal conditions and relies on several approximations and simplifications. The omitting of all non-ideal effects when analysing a non-uniform velocity profile has to be acknowledged and, if needed, rectified in more advanced models. Also the use of the same velocity profile throughout the entire ESP represents a significant simplification, which should be scrutinized in a refined analysis. For the study of electrode misalignment, similar simplifications occur, as well as the use of the rather inaccurate expression for migration velocity in terms of electric field strengths, gas viscosity and particle size. Finally, the correction for premature sparking at the minimum electrode distance assumes that sparks never occur between frames and support structures in the ESP, which is not always the case.

References

[1] White H., *Industrial Electrostatic Precipitation*. Addison-Wesley, 1963.

[2] Oglesby Jr., S., Nichols G. B., *Electrostatic Precipitation*. Marcel Dekker, 1978.

[3] Parker K.R., *Applied Electrostatic Precipitation*. Chapman & Hall, 1997.

[4] Burton C.L., Smith D.A., *Journal of the Air Pollution Control Association* 25, (1975), pp. 139-143.

[5] Rosby S-O., *Flakt Engineering* 1, (1977), No. 4 pp. 1-4.

[6] Brown D.M., Shilling N.Z., in *Proc. 1st Int. Conf. on Electrostatic Precipitation*, Monterey CA, USA, Oct. 14-16 (1981), pp. 145-177.

[7] Lind L., in *Proc. 6th Symposium on the Transfer and Utilization of Particulate Control Technology vol.2*, New Orleans LA, USA, Feb. 25-28 (1986), pp. 33:1-33:15.

[8] Jedrusik M., Sarna M., in *Proc. 6th Int. Conf. on Electrostatic Precipitation*, Budapest, Hungary, June 18-21 (1996), pp. 184-189.

[9] Lee G.M., *et al.*, in *Proc. 7th Int. Conf. on Electrostatic Precipitation*, Kyongju, Korea, Sep. 20-25 (1998), pp. 457-464.

[10] Andersson C., Lind L., in *Proc. 8th Int. Conf. on Electrostatic Precipitation*, Birmingham AL, USA, May 14-17 (2001), paper A5-1.

[11] Jedrusik M., Swierczok A., Nowaczewski E., Sarna M., Grys E., in *Proc. 8th Int. Conf. on Electrostatic Precipitation*, Birmingham AL, USA, May 14-17 (2001), paper A5-2.

[12] Yamamoto T., Velkoff H.R., *Journal of Fluid Mechanics* 108, (1981), pp. 1-18.

[13] Shaughnessy E.J., Davidson J.H., Hay J.C., *Aerosol Science and Technology* 4, (1985), pp. 471-476.

[14] Halldin C., Håkansson R., Johansson L-E., Porle K., in *Proc. 6th Int. Conf. on Electrostatic Precipitation*, Budapest, Hungary, June 18-21 (1996), pp. 406-416.

[15] Chang J.S., Urashima K., *International Journal of Plasma Environmental Science and Technology* 3, (2009), pp. 138-141.

[16] Hein A.G., *Journal of the Air Pollution Control Association* 39, (1989), pp. 766-771.

[17] Gibson D., Schmitz W., Hein A.G., in *Proc. 7th Int. Conf. on Electrostatic Precipitation*, Kyongju, Korea, Sep. 20-25 (1998), pp. 188-195.

[18] Boyd M., in *Proc. 8th Int. Conf. on Electrostatic Precipitation*, Birmingham AL, USA, May 14-17 (2001), paper A5-3.

[19] Sarna M., Sladkowska-Rybka B., Grys E., in *Proc. 9th Int. Conf. on Electrostatic Precipitation*, Mpumalanga, South Africa, May 17-21 (2004), paper D-08.

[20] ICAC - Institute of Clean Air Companies, *ICAC-EP-7 Electrostatic Precipitator Gas Flow Model Studies*. ICAC, 2004.

[21] Matts S., Öhnfeldt P-O., *SF Review* 6-7, (1964), pp. 103-122.